Available online at www.sciencedirect.com
ScienceDirect
Journal of Nuclear Materials 363–365 (2007) 72–77
journal of nuclear materials
www.elsevier.com/locate/jnucmat

Transport and deposition of ^{13}C from methane injection into partially detached H-mode plasmas in DIII-D

W.R. Wampler [a,*], A.G. McLean [b], S.L. Allen [c], N.H. Brooks [d], J.D. Elder [c], M.E. Fenstermacher [c], M. Groth [c], P.C. Stangeby [b], W.P. West [d], D.G. Whyte [e]

[a] *Sandia National Laboratories, Albuquerque, NM 87185, USA*
[b] *University of Toronto Institute for Aerospace Studies, Toronto, Canada M3H 5T6*
[c] *Lawrence Livermore National Laboratory, Livermore, CA 94550, USA*
[d] *General Atomics, San Diego, CA 92186-5608, USA*
[e] *University of Wisconsin, Madison, WI 53706, USA*

Abstract

Experiments are described which examine the transport and deposition of carbon entering the main plasma scrape-off layer in DIII-D. $^{13}CH_4$ was injected from a toroidally symmetric source into the crown of lower single-null partially detached ELMy H-mode plasmas. ^{13}C deposition, mapped by nuclear reaction analysis of tiles, was high at the inner divertor but absent at the outer divertor, as found previously for low-density L-mode plasmas. This asymmetry indicates that ionized carbon is swept towards the inner divertor by a fast flow in the scrape-off layer. In the private flux region between inner and outer strike points, carbon deposition was low for L-mode but high for the H-mode plasmas. OEDGE modeling reproduces observed deposition patterns and indicates that neutral carbon dominates deposition in the divertor from detached H-mode plasmas.

PACS: 52.40.Hf; 52.55.Fa; 28.52.Fa

Keywords: DIII-D; $^{13}CH_4$ injection; Nuclear reaction analysis; Erosion/deposition; Impurity transport

1. Introduction

Plasma interactions with carbon plasma-facing components in the main plasma chamber are a source of hydrocarbons to the plasma scrape-off layer where they dissociate and ionize. Some of this carbon will deposit near its origin during the molecular breakup process, and some will be incorporated as ions into the SOL plasma and will deposit elsewhere along with deuterium or tritium. The rate of carbon erosion and where it deposits impact tritium retention and strategies for its mitigation. Previous studies of erosion and deposition in the DIII-D divertor have concluded that with detached divertor plasmas, there is net deposition of carbon everywhere in the divertor and that the main plasma chamber is the probable source of this carbon [1,2].

* Corresponding author. Tel.: +1 505 844 4114; fax: +1 505 844 7775.
E-mail address: wrwampl@sandia.gov (W.R. Wampler).

0022-3115/$ - see front matter © 2007 Elsevier B.V. All rights reserved.
doi:10.1016/j.jnucmat.2006.12.038

Here we report experiments which examine the transport and deposition of carbon entering the main plasma scrape-off layer. $^{13}CH_4$ was injected into partially detached divertor (PDD) ELMy H-mode plasmas. Partially detached divertor plasmas are planned for ITER to reduce fluxes of particles and heat [3]. Results are compared with a previous study in which $^{13}CH_4$ was injected into low-density L-mode plasmas in DIII-D [4,5]. In both experiments, the $^{13}CH_4$ was injected from a toroidally symmetric source into the crown of lower single-null plasmas. This plasma geometry, and a location of injection far from the divertor, were chosen to simulate hydrocarbons originating from plasma interaction with carbon on the main chamber wall. Nuclear reaction analysis was used to map the resulting coverage of ^{13}C on carbon tiles removed from the vessel. The fact that the carbon deposition occurred during identical and well diagnosed plasmas allows comparison with models of impurity transport and deposition [6,7]. Conclusions about mechanisms controlling carbon transport and deposition, and implications for tritium retention are discussed.

2. Experimental procedure

$^{13}CH_4$ was injected at a steady rate into 17 identical lower single-null plasmas. Fig. 1 shows an overlay of plasma current and core electron density and temperature as measured by Thomson scattering for all discharges. Neutral beam heating at 6.6 MW produced H-mode plasmas with edge localized mode (ELM) characteristics at a constant frequency of 200 Hz. Partially detached divertor conditions were obtained by deuterium gas puffing. The line-average electron density was $8 \times 10^{19}\,m^{-3}$. The inner strike point (ISP) and outer strike point (OSP) were positioned on the divertor floor at major radii of 1.251 and 1.643 m respectively, and were held fixed to within approximately ± 0.5 cm.

Divertor Langmuir probes show little plasma contact with the divertor at the ISP, but more plasma contact outboard of the OSP. Heat flux to the divertor, determined by infrared imaging, is greater at the OSP than at the ISP but reduced and broadened typical of detached plasma conditions. Time resolved imaging using tangential viewing cameras show that emission from deuterium and carbon in the divertor are modulated by the ELMs. Radiation intensity is low at the strike points between ELMs, consistent with detached plasmas,

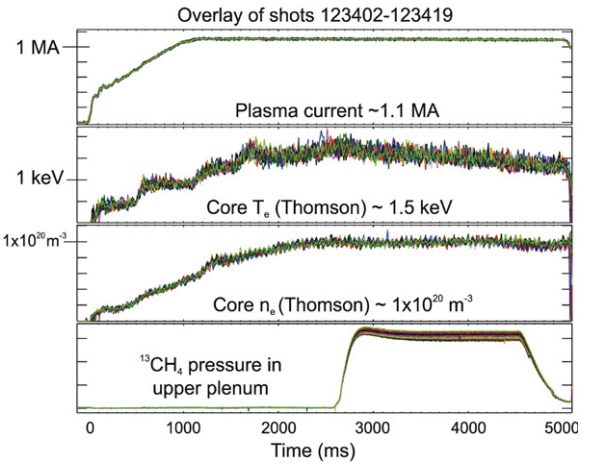

Fig. 1. Overlays of plasma current and core electron density and temperature as measured by Thomson scattering, and pressure in the upper pumping plenum for the plasmas in the $^{13}CH_4$ injection shots.

but increases during the ELMs. Maps of emission intensity from CH (431.0 nm) CII (514.7 nm) and CIII (465.0) nm, were obtained from 2D reconstruction of tangential viewing camera images of the upper chamber during methane injection into L-mode and detached H-mode plasmas. Comparing emission from CH, CII and CIII, the emission from the more highly ionized states was (a) closer to the separatrix for both L- and H-mode, and (b) shifted poloidally towards the inner divertor for L-mode but not for H-mode. The emission was farther from the separatrix for H-mode than for L-mode, presumably indicating earlier dissociation and ionization by the denser H-mode plasma. Divertor Thomson scattering (DTS) shows that the outboard divertor plasma is very cold and dense, with $T_e < 5$ eV, radially outward from the strike-point into the far SOL, and from the divertor target up to about the X-point in height, with no significant gradients in density or temperature across the outer divertor separatrix into the private flux region.

$^{13}CH_4$ was injected from the upper pumping plenum (illustrated in Fig. 3) providing a high degree of toroidal symmetry to the $^{13}CH_4$ flow into the plasma [5]. The $^{13}CH_4$ was injected for 2 s intervals during partially detached H-mode conditions, at a nearly constant rate of 18.8 ± 0.3 torr l/s or $0.665 \pm 0.01 \times 10^{21}$ ^{13}C atoms/s, chosen to be as high as possible without significantly perturbing the core or divertor plasma conditions. The $^{13}CH_4$ injection was repeated for 17 consecutive identical

plasmas, for a total of 2.3×10^{22} atoms of injected ^{13}C. The quantity of ^{13}C injected was 2.3 times larger in this study than in the previously reported study with L-mode plasmas [4]. Helium glow discharge conditioning was done between shots, however, residual gas analysis showed that this removed less than 1% of the injected ^{13}C. The $^{13}CH_4$ injection experiment was done on the last day of the campaign, and no baking or cleaning was performed afterwards. At the beginning of the subsequent machine vent, 64 carbon tiles were removed for analysis. The set included 49 tiles within $\pm 15°$ of the same toroidal angle. To check toroidal symmetry, six tiles were included from toroidally opposite locations but the same poloidal angles as tiles from the main toroidal set.

^{13}C coverage on the tiles was measured at Sandia National Laboratories by nuclear reaction analysis using the $^{13}C(^3He,p)^{15}N$ reaction as described in Ref. [4]. The total uncertainty in the measurements of ^{13}C coverage is estimated to be $\pm 2 \times 10^{16}$ atoms/cm^2. Thus the lowest detectable ^{13}C deposition is about 2×10^{16} atoms/cm^2. For comparison, the injected quantity of ^{13}C distributed uniformly over the wall of DIII-D would give a coverage of about 2×10^{16} atoms/cm^2. The measurement integrates the ^{13}C within about 0.6 μm of the surface which includes the thinner surface layer containing the deposited ^{13}C.

Proton induced gamma emission (PIGE), using the $^{13}C(p,\gamma)N^{14}$ reaction, was done at the University of Wisconsin on selected tiles. This method uses a narrow resonance for protons at 1.748 MeV giving a 9.17 MeV gamma (γ). This measures the concentration of ^{13}C versus depth with a smaller depth resolution and hence lower detection limit for ^{13}C deposited on graphite of about 10^{15} atoms/cm^2. PIGE profiling showed enrichments of ^{13}C concentrations from a few percent to a few tens of percent in layers containing up to a few times 10^{18} atoms/cm^2 corresponding to a thickness of a few tenths of a micron for graphite.

3. ^{13}C deposition

^{13}C coverage was measured by ^{3}He,p NRA along scans in the poloidal direction through the center, and near the edges of each tile. Three additional scans were done along the toroidal direction on most of the center column tiles. In nearly all cases the ^{13}C distribution was similar for the various poloidal scans on a given tile, and for tiles from the same poloidal position but at different toroidal angles, indicating that the ^{13}C deposition was toroidally symmetric.

Fig. 2 shows ^{13}C coverage measured by ^{3}He,p NRA versus poloidal position on tiles from the H-mode experiment. Deposition was heaviest in the lower divertor, but also measurable on ceiling tiles near the region of injection. ^{13}C deposition on all other regions, including center column tiles and outer wall and limiter tiles, was below the limit of detection by ^{3}He,p NRA. Fig. 3 shows an expanded view of ^{13}C coverage measured on the ceiling tiles for both L- and H-mode experiments. The top panel shows the locations of the tiles and magnetic field contours. In the H-mode experiment, about 0.5×10^{17}/cm^2 of ^{13}C deposition was observed on tiles 52 and 53 adjacent to the opening through which the $^{13}CH_4$ was injected. Elsewhere, and on the tiles from the L-mode experiment, the ^{13}C deposition was at or below the limit of detection by the ^{3}He,p NRA method, however PIGE showed about 2×10^{16} ^{13}C/cm^2 on tiles 51 and 53 from the L-mode experiment. These measurements show that in the H-mode experiment about 8% to 10% of the injected ^{13}C is deposited locally, probably as neutral hydrocarbon fragments, during dissociation of the $^{13}CH_4$. The remainder is presumably ionized and transported by the scrape-off layer plasma to more distant locations.

Fig. 4 shows an expanded view of ^{13}C deposition in the lower divertor. For both L-mode and H-mode plasmas, ^{13}C coverage was high inboard of the inner

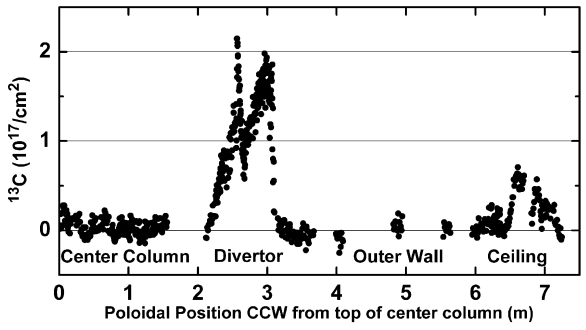

Fig. 2. The circles show the ^{13}C coverage measured by ^{3}He,p NRA on tiles from the H-mode experiment, averaged over the various scans on each tile. The horizontal coordinate is the distance along the tile surfaces down the center column, out across the floor, up the outer wall and in across the ceiling. Negative values of ^{13}C deposition plotted in Fig. 3 are due to inaccuracies in subtraction of background, and are within the estimated uncertainty of the measurement.

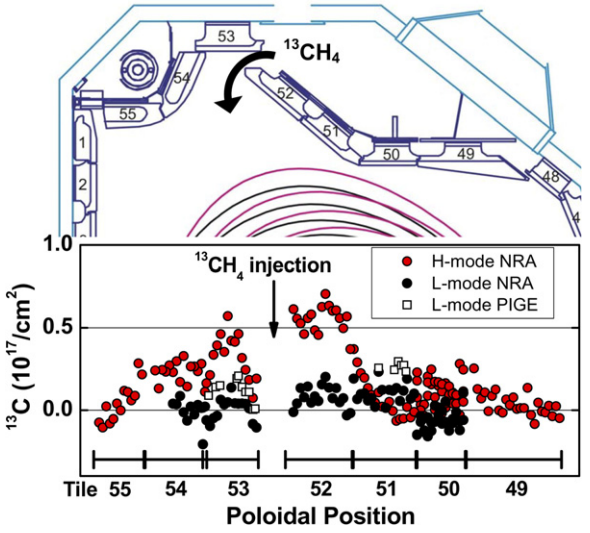

Fig. 3. The bottom panel shows an expanded view of ^{13}C coverage on the ceiling tiles for H-mode (red) and L-mode (black) measured by ^{3}He,p NRA (circles) and PIGE (squares). The positions of the ISP and OSP where the separatrix intersects the divertor, are indicated. The top panel shows the locations of the tiles and magnetic field contours, black for L-mode and red for H-mode. (For interpretation of the references in colour in this figure legend, the reader is referred to the web version of this article.)

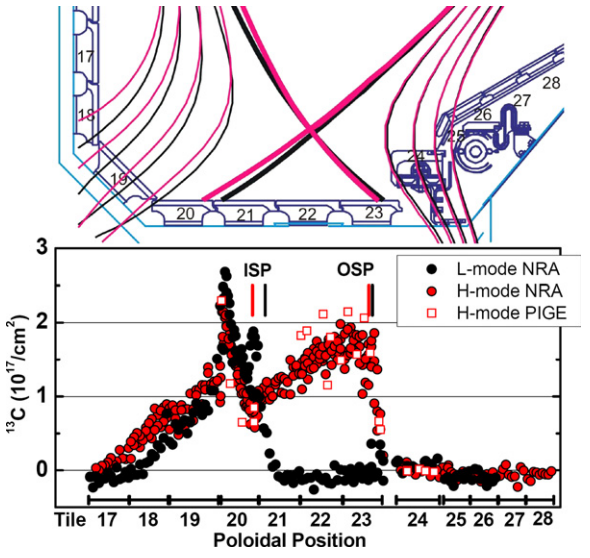

Fig. 4. The bottom panel shows an expanded view of ^{13}C coverage on the lower divertor tiles for H-mode (red) and L-mode (black) measured by ^{3}He,p NRA. The positions of inner and outer strike points for the L and H-mode are indicated. The top panel shows the locations of the tiles and magnetic field contours, black for L-mode and red for H-mode. (For interpretation of the references in colour in this figure legend, the reader is referred to the web version of this article.)

strike point, and low at the outer divertor. In the private flux region between inner and outer strike points, carbon deposition was low for L-mode but high for the H-mode plasmas. For H-mode, about 13% of the injected ^{13}C was deposited at the inner divertor and about 24% in the private flux region. For the L-mode, about 30% of the injected ^{13}C was deposited at the inner divertor and very little in the private flux region. PIGE measurements of ^{13}C deposition in the divertor from H-mode (Fig. 4) agreed with ^{3}He,p NRA results, and also showed no deposition at the outer divertor above the lower detection limit of $\sim 10^{15}$ atoms/cm^2. Thus the asymmetry in ^{13}C deposition at inner and outer divertors is greater than two orders of magnitude. $^{13}CH_4$ injection into L-mode plasmas in JET also resulted in ^{13}C deposition at the inner divertor but not at the outer divertor [8].

In both L-mode and H-mode experiments, approximately 30–40% of the injected ^{13}C was deposited in the lower divertor, and about 10% near the region of injection. The fate of the remaining 50–60% is not yet established. Although ^{13}C coverage on plasma-facing surfaces of the center column tiles was below the detection limit of ^{3}He,p NRA (see Fig. 1), significant amounts might be present at lower coverage over a large area. Also, PIGE measurements indicate that ^{13}C was deposited on a leading edge of one of the center column tiles from the L-mode experiment. The total amount of ^{13}C deposited on the center column is uncertain but could be a significant fraction of the injected quantity.

4. Discussion

4.1. Carbon deposition from detached H-Mode, DiMES and $^{13}CH_4$ injection experiments

Measurements of carbon deposition in the lower divertor of DIII-D with lower single-null detached ELMy H-mode plasmas have been reported previously [1,2]. Those measurement were done using the divertor materials evaluation system (DiMES). Net deposition was found at the ISP and OSP, with deposition decreasing abruptly outside the OSP, very similar to the pattern of ^{13}C deposition found in the present study with detached H-mode plasmas. It was concluded that the source of carbon must lie outside the divertor. In the DiMES experiments, net deposition rates at the ISP and OSP were observed to be 1×10^{16} carbon atoms/cm^2 s and 2×10^{16}

carbon atoms/cm^2 s respectively. For comparison, the rates of ^{13}C deposition observed from $^{13}CH_4$ injection into detached H-mode plasmas were 0.25×10^{16} atoms/cm^2 s and 0.5×10^{16} atoms/cm^2 s respectively at the ISP and OSP. These values were obtained by dividing the observed deposition at the strike points (see Fig. 4) by the total time of $^{13}CH_4$ injection (2 s per shot for 17 shots). Thus the total rate of carbon deposition in the DiMES experiments was approximately four times larger than the rate of ^{13}C deposition in the injection experiment. Assuming the plasmas were similar in the two experiments, we infer that the source of carbon from plasma interactions with the wall is about four times the rate of $^{13}CH_4$ injection or 3×10^{21} atoms (0.06 g) per second. The films deposited from detached plasmas in DIII-D were experimentally observed [1] to have $D/C = 1$ as expected for codeposition by low energy neutrals from cold dense plasmas. The rate of deuterium retention by codeposition is therefore also about 3×10^{21} atoms/s or 36 g/h of plasma.

4.2. OEDGE modeling

The onion skin model EIRENE DIVIMP edge code (OEDGE) has been used to model the breakup, transport and deposition of ^{13}C for both the low density L-mode [6] and detached H-mode plasmas [9]. The H-mode simulations show three key features that are necessary to reproduce the pattern of deposition observed in the H-mode experiment. First, a fast parallel flow ($M \sim 0.3$) toward the inner divertor in the scrape-off layer is required to obtain deposition at the inner divertor as observed. Second, a radial pinch is required to transport the ^{13}C toward the separatrix. Without this pinch the fast breakup and ionization of the $^{13}CH_4$ near the puff location deposits too many ^{13}C ions on the inner wall and deposits those that reach the divertor too far from the inner strike point with little deposition on the private flux zone (PFZ) wall. Third, the H-mode plasma was deeply detached with cold, dense plasma extending along the inner plasma leg to the *X*-point and in the PFZ. This cold dense plasma results in strong volume recombination of ^{13}C ions in the *X*-point region and directly leads to deposition on the PFZ wall.

The observation, that carbon deposits in the private flux region from detached H-mode plasmas but not from L-mode plasmas, is a key result. OEDGE modeling indicates that the cause of this difference is the greater extent of the cold dense detached divertor plasma in H-mode and resulting shift in the location where parallel flow stops and volume recombination occurs [9]. According to the modeling, this region is near the inner divertor target for the low-density L-mode but is near the *X*-point for detached H-mode. The radial pinch transporting carbon towards the separatrix, together with volume recombination near the *X*-point allows carbon neutrals to deposit in the private flux region. The influence of ELMs on transport and deposition of carbon in the detached H-mode plasma is presently not yet resolved but is being investigated [9].

5. Conclusions

Injection of methane at the top of lower single-null plasmas in DIII-D provides a simulation of hydrocarbons entering the scrape-off layer from plasma interactions with the main chamber wall. Use of $^{13}CH_4$ allows mapping of the resulting carbon deposition by nuclear reaction analysis of tiles. The observed ^{13}C deposition from detached H-mode plasmas is consistent with previous studies using DiMES. From measured rates of carbon deposition in the DiMES and $^{13}CH_4$ injection experiments, the rate of carbon erosion and codeposition was estimated to be 0.06 g/s. In a long pulse DT fueled machine, tritium inventory from this rate of codeposition would soon constrain operation. This illustrates the need to develop efficient methods for recovering tritium from codeposits, or else to avoid main chamber sources of carbon, for example by using metal instead of a carbon wall, in such machines.

Comparison between observed deposition patterns and models provides new insight into physical processes controlling carbon deposition and hence deuterium or tritium accumulation by codeposition. The picture that emerges from this comparison is that in both low-density L-mode and PDD H-mode plasmas, most of the carbon is promptly ionized and is swept towards the inner divertor by a fast parallel flow in the SOL. This flow results in high deposition at the inner divertor and low deposition at the outer divertor for both L-mode and PDD H-mode plasmas. Modeling indicates that carbon deposits from detached PDD H-mode mainly as neutrals formed by volume recombination. High deposition in the private flux region from PDD H-mode but not from L-mode plasmas results from the greater extent of

the detached plasma in H-mode and the resulting shift in the region of carbon recombination from the outer target towards the *X*-point. The conclusion that carbon deposits as neutrals from detached plasmas has important implications for tritium retention and strategies for its mitigation. Such deposition occurs in regions shadowed from ion flux and is not easily removed by plasma conditioning. However it should now be possible to predict locations of codeposition from detached plasmas and optimize the divertor geometry to minimize tritium accumulation in inaccessible regions.

Acknowledgements

The authors thank Stuart Van Deusen for his NRA measurements of ^{13}C coverage on the tiles, and Chris Chrobak, Josh Shea and Kevin Christie for the PIGE measurements. Sandia is a multiprogram laboratory operated by Sandia Corporation, a Lockheed Martin Company, for the US Department of Energy. This work was supported by the US Department of Energy under Contract Nos. W-7405-ENG-48, DE-FC02-04ER54698, DE-FG02-04ER54762 and DE-AC04-95ER85000.

References

[1] W.R. Wampler, D.G. Whyte, C.P.C. Wong, W.P. West, J. Nucl. Mater. 290–293 (2001) 346.
[2] D.G. Whyte, W.P. West, C.P.C. Wong, R. Bastasz, J.N. Brooks, W.R. Wampler, N.H. Brooks, J.W. Davis, R.P. Doerner, A.A. Haasz, R.C. Isler, G.L. Jackson, R.G. Macaulay-Newcomb, M.R. Wade, Nucl. Fusion 41 (2001) 1243.
[3] IAEA, Report No. 24, 2002.
[4] W.R. Wampler, S.L. Allen, A.G. McLean, W.P. West, J. Nucl. Mater. 337–339 (2005) 134.
[5] S.L. Allen, W.R. Wampler, A.G. McLean, D.G. Whyte, W.P. West, P.C. Stangeby, N.H. Brooks, D.L. Rudakov, V. Phillips, M. Rubel, G.F. Matthews, A. Nagy, R. Ellis, A. Bozek, J. Nucl. Mater. 337–339 (2005) 30.
[6] J.D. Elder, P.C. Stangeby, D.G. Whyte, S. Allen, A. McLean, J. Boedo, B.D. Bray, N.H. Brooks, M.E. Fenstermacher, M. Groth, C. Lasnier, S. Lisgo, D.L. Rudakov, W.R. Wampler, J.G. Watkins, W.P. West, J. Nucl. Mater. 337–339 (2005) 79.
[7] A.G. McLean, J.D. Elder, P.C. Stangeby, S.L. Allen, J.A. Boedo, N.H. Brooks, M.E. Fenstermacher, M. Groth, S. Lisgo, A. Nagy, D.L. Rudakov, W.R. Wampler, J. Watkins, W.P. West, D.G. Whyte, J. Nucl. Mater. 337–339 (2005) 124.
[8] J.P. Coad et al., Nucl. Fusion 46 (2006) 350.
[9] J.D. Elder et al., in: Proceedings of the 17th International Conference on Plasma Surface Interactions in Controlled Fusion Devices, 2006.